International Conference on Mathematics, Computational Methods & Reactor Physics (M&C 2009)
Saratoga Springs, New York, May 3-7, 2009, on CD-ROM, American Nuclear Society, LaGrange Park, IL (2009)

ANALYSIS AND NUMERICAL SOLUTION FOR MULTI-PHYSICS COUPLING OF NEUTRON DIFFUSION AND THERMOMECHANICS IN SPHERICAL FAST BURST REACTORS

Samet Y. Kadioglu and Dana A. Knoll
Multipysics Methods Group
Reactor Physics Analysis and Design
Idaho National Laboratory
P. O. Box 1625, MS 3840, Idaho Falls, ID 83415
samet.kadioglu@inl.gov; dana.knoll@inl.gov

Cassiano de Oliveira
Chemical and Nuclear Engineering Department
The University of New Mexico
Albuquerque, NM 87131-1341
cassiano@unm.edu

ABSTRACT

Coupling neutronics to thermomechanics is important for the analysis of fast burst reactors, because the criticality study of fast burst reactors depends on the thermomechanical behavior of fuel materials. For instance, the shut down mechanism or the transition between super and sub-critical states are driven by the fuel material expansion or contraction. The material expansion or contraction is due to the temperature gradient which results from fission power. In this paper, we introduce a numerical model for coupling of neutron diffusion and thermomechanics in fast burst reactors. We perform non-dimensional analysis of the coupled system which provides insight into the behavior of the transient. We studied material behavior corresponding to different levels of reactivity insertion.

Key Words: Multi-physics Analysis, Fast Burst Reactors,Numerical Coupling Models, Non-dimensional Analysis

1. INTRODUCTION

There has been a long standing interest in developing numerical models for the analysis of fast burst critical experiments. For example, in an early model [1] the uncoupled thermomechanics of fissile materials was studied by inserting prescribed temperature fields into the elastic equations. More recently, a model was developed [2] which coupled thermomechanics of a fast burst reactor with point reactor kinetics. Here, we present a model which fully couples spatially-dependent neutron diffusion and thermomechanics in order to simulate transient behavior of a fast burst criticality excursion.

The problem involves solving a set of non-linear differential equations which approximate neutron diffusion, temperature change, and material behavior. With this equation set it is possible to model the transition from a supercritical to subcritical state and corresponding material response, e.g, possible mechanical vibration.

We present results from a one-group, spherically symmetric diffusion model accounting for prompt neutrons only. We don’t include delayed neutrons, since the time scales involved are too

fast in order for delayed neutrons to contribute to the system. We also ignore thermal conduction or thermal surface radiation cooling.

The present paper is organized as follows. In Section 2, we describe the model equations and their dimensionless forms. In Section 3, we describe our numerical procedure to the coupled system. In Section 4, we present our computational results and analysis. Section 5 contains our concluding remarks.

2. GOVERNING EQUATIONS

Our model equations are formulated in a spherically symmetric coordinates [1–3]. In this case, the neutron diffusion is governed by

$$\frac{1}{v}\frac{\partial \phi}{\partial t} - \frac{1}{r^2}\frac{\partial}{\partial r}[r^2 \frac{1}{3N\sigma_{tr}}\frac{\partial \phi}{\partial r}] + [N\sigma_a - \nu N\sigma_f]\phi = 0. \tag{1}$$

The temperature field is evolved with

$$\rho c_p \frac{\partial T}{\partial t} - \omega N \sigma_f \phi = 0. \tag{2}$$

The material displacement is modeled by the following elastic wave equation;

$$\frac{1}{c^2}\frac{\partial^2 u}{\partial t^2} - [\frac{\partial^2 u}{\partial^2 r} + \frac{2}{r}\frac{\partial u}{\partial r} - \frac{2}{r^2}u] + \frac{1+\upsilon}{1-\upsilon}\beta\frac{\partial T}{\partial r} = 0. \tag{3}$$

The material density is computed by considering the mass/particle conservation in a spherical domain;

$$\rho = \rho_0 [\frac{r}{r+u}]^3. \tag{4}$$

Finally, we give a formula for the radial stress component[1]

$$\tau_r = \frac{\epsilon}{(1+\upsilon)(1-2\upsilon)}[2\upsilon\frac{u}{r} + (1-\upsilon)\frac{\partial u}{\partial r} - (1+\upsilon)\beta T]. \tag{5}$$

Formula (5) will serve as a surface boundary condition when solving Eq. (3).

We remark that there are limitations for this coupling model. For instance, the diffusion model is not the most accurate model to evaluate neutron flux (e.g, one can implement more accurate transport theory for this purpose). Nevertheless, this model is sufficient enough to couple with the thermomechanics to obtain preliminary material behaviors which are observed experimentally. Secondly, the linear mechanics model (elastic wave model) is fine for small material displacements. However, one has to use a non-linear mechanics model (e.g, time dependent hydrodynamics equations) in order to solve large material displacements.

The unknowns and constant parameters that appear in these equations are defined as

ϕ : Neutron flux
T : Temperature
u : Material displacement
ρ : Material density
r : Spatial variable
t : Time variable
v : Average neutron speed
N : Number atom density

ν : Number of neutron produced per fission
σ_{tr} : Microscopic transport cross section
σ_a : Microscopic absorption cross section
σ_f : Microscopic fission cross section
ω : Amount of average energy released per fission
c_p : Specific heat
β : Linear thermal expansion coefficient
$c = [\frac{(1-\upsilon)\epsilon}{(1+\upsilon)(1-2\upsilon)\rho}]^{1/2}$: Wave speed
υ : Poisson's ratio
ϵ : Young's modulus

We note that the material density can be written as the product of the number atom density and the atomic mass, i.e, $\rho = NAm$.

2.1. Dimensionless Form

In this section, we introduce several non-dimensional parameters and write down the dimensionless form of Eqs. (1), (2), and (3). We consider the following dimensionless group;

$$\begin{aligned} \tilde{r} = \frac{r}{R_0}, \;\; \tilde{t} = \frac{t}{\frac{l}{k-1}}, \;\; \tilde{\phi} &= \frac{\phi}{\phi_0}, \;\; \tilde{T} = \frac{T}{T_0}, \\ \tilde{u} &= \frac{u}{R_0}, \;\; \tilde{\rho} = \frac{\rho}{\frac{Am}{R_0\sigma_{tr}}} \end{aligned} \tag{6}$$

where R_0 is the initial radius of the sphere, ϕ_0 is the maximum initial neutron flux, T_0 is the maximum initial temperature, $l = [v\Sigma_a(1 + L^2Bg^2)]^{-1}$ is the mean lifetime of neutron in the reactor, $\Sigma_a = N\sigma_a$ is the macroscopic absorption cross section, $L^2 = \frac{D}{\Sigma_a}$ is the diffusion area, $D = \frac{1}{3\Sigma_{tr}}$ is the diffusion coefficient, $\Sigma_{tr} = N\sigma_{tr}$ is the macroscopic transport cross section, $Bg^2 = (\frac{\pi}{R_0})^2$ is the geometric buckling, $\Sigma_f = N\sigma_f$ is the macroscopic fission cross section, and $k = \frac{\nu\Sigma_f/\Sigma_a}{1+L^2Bg^2}$ is the multiplication factor. We note that k represents the initial multiplication factor which corresponds to a supercritical reactor state. In other words, the system is always set to a supercritical state so that we avoid singularities in the non-dimensional equations due to division by the $(k-1)$ term. With these, we have the following non-dimensional system of equations

$$\frac{\partial\tilde{\phi}}{\partial\tilde{t}} - P\frac{1}{\tilde{r}^2}\frac{\partial}{\partial\tilde{r}}[\tilde{r}^2\frac{1}{3\tilde{\rho}}\frac{\partial\tilde{\phi}}{\partial\tilde{r}}] + P\frac{[\sigma_a - \nu\sigma_f]}{\sigma_{tr}}\tilde{\rho}\tilde{\phi} = 0, \tag{7}$$

$$\frac{\partial\tilde{T}}{\partial\tilde{t}} - C\tilde{\phi} = 0, \tag{8}$$

$$\frac{1}{\tilde{c}^2}\frac{\partial^2\tilde{u}}{\partial\tilde{t}^2} - [\frac{\partial^2\tilde{u}}{\partial^2\tilde{r}} + \frac{2}{\tilde{r}}\frac{\partial\tilde{u}}{\partial\tilde{r}} - \frac{2}{\tilde{r}^2}\tilde{u}] + \frac{1+\upsilon}{1-\upsilon}\beta T_0\frac{\partial\tilde{T}}{\partial\tilde{r}} = 0, \tag{9}$$

where $P = \frac{vl}{R_0(k-1)}$ and $C = \frac{l\omega\sigma_f\phi_0}{T_0(k-1)c_pAm}$ are dimensionless parameters, and $\tilde{c} = \frac{c}{\frac{R_0(k-1)}{l}}$ is the dimensionless wave speed.

When we implement the surface boundary condition for the displacement, we set $\tau_r = 0$, thus the non-dimensionalization of Eq. (5) becomes

$$2\upsilon\tilde{u} + (1-\upsilon)\frac{\partial\tilde{u}}{\partial\tilde{r}} = (1+\upsilon)T_0\beta\tilde{T}. \tag{10}$$

More details about the non-dimensionalization procedure are given in [4].

3. NUMERICAL METHOD

Our numerical algorithm consists of an explicit and an implicit block. The reason why we develop this kind of approach is that the time steps are impractically small(e.g, due to the stiffness of the problem) if one wants to solve Eq. (1) explicitly. Therefore, we make use of an implicit strategy to solve Eqs. (1) and (2). On the other hand, it is well known that wave equations are solved by following the characteristic wave speed due to numerical instability and accuracy issues. This requires explicitly obeying the so called Courant stability conditions [5]. Therefore, an explicit scheme is better choice for solving Eq. (3).

The numerical algorithm is executed as follows. First, Eq. (3) is advanced with a second order explicit discretization in time to obtain a new displacement (the density field is immediately updated by Eq. (4)). Then the updated density is inserted into the implicit loop to advance Eqs. (1) and (2) which is also second order accurate in time. All of the spatial terms are discretized by second order differencing schemes. Therefore, the resulting overall simulation will be shown to be second order accurate in space and time.

We note that our algorithm implementation looks like an operator split scheme (e.g, thermomechanics is operator split from the neutronics). Thus, one may think that it is first order in time. However, the time discretization of the wave equation is centered around time level *n* so that overall scheme produces second order time values. We note that the algorithm can be implemented in another way. In other words, the explicit block can be called within the implicit loop as a function evaluation. We have considered both implementations and both are second order accurate in time, but the former is computationally more expensive.

Here, we attribute our second order results to our specific model (linear mechanics model). However, if one wants to solve hydrodynamics model (non-linear mechanics model) with our explicit-implicit strategy, the results will be first order in time due to splitting errors. In this case, one has to implement a truly non-linearly consistent algorithm. This issue is currently being investigated.

Below, we briefly describe our explicit and implicit blocks.

3.1. Explicit Block

The explicit block for solving Eq. (9) together with Eq. (10) is based on a second order centered in time and space scheme[5],

$$\begin{aligned}\frac{\tilde{u}_i^{n+1} - 2\tilde{u}_i^n + \tilde{u}_i^{n-1}}{\Delta\tilde{t}^2} &= \tilde{c}_i^n\{\frac{\tilde{u}_{i+1}^n - 2\tilde{u}_i^n + \tilde{u}_{i-1}^n}{\Delta\tilde{r}^2} \\ + \quad \frac{2}{\tilde{r}_i}\frac{\tilde{u}_{i+1}^n - \tilde{u}_{i-1}^n}{2\Delta\tilde{r}} &- \frac{2}{\tilde{r}_i^2}\tilde{u}_i^n - \frac{1+\upsilon}{1-\upsilon}\beta T_0\frac{\tilde{T}_{i+1}^n - \tilde{T}_{i-1}^n}{2\Delta\tilde{r}}\}\end{aligned} \tag{11}$$

Here the index i represents i^{th} cell, and n denotes the current time level.

3.2. Implicit Block

Our implicit block solves Eqs. (7) and (8) based on the so called *theta*-scheme. For instance

$$\mathbf{U}_i^{n+1} = \mathbf{U}_i^n + \Delta\tilde{t}[\theta\mathbf{F}_i^n + (1-\theta)\mathbf{F}_i^{n+1}], \tag{12}$$

where $\mathbf{U} = (\tilde{\phi}, \tilde{T})$, $\mathbf{F} = (F_{\tilde{\phi}}, F_{\tilde{T}})$,

$$\begin{aligned} F_{\tilde{\phi},i} &= P\frac{1}{\tilde{r}_i^{\,2}}\frac{\partial}{\partial\tilde{r}}[\tilde{r}^2\frac{1}{3\tilde{\rho}}\frac{\partial\tilde{\phi}}{\partial\tilde{r}}]_i - P\frac{[\sigma_a - \nu\sigma_f]}{\sigma_{tr}}\tilde{\rho}_i\tilde{\phi}_i, \\ F_{\tilde{T},i} &= C\tilde{\phi}_i \end{aligned} \tag{13}$$

where $\frac{\partial}{\partial\tilde{r}}[\tilde{r}^2\frac{1}{3\tilde{\rho}}\frac{\partial\tilde{\phi}}{\partial\tilde{r}}]_i = \frac{(\tilde{r}^2\frac{1}{3\tilde{\rho}}\frac{\partial\tilde{\phi}}{\partial\tilde{r}})_{i+1/2} - (\tilde{r}^2\frac{1}{3\tilde{\rho}}\frac{\partial\tilde{\phi}}{\partial\tilde{r}})_{i-1/2}}{\Delta\tilde{r}}$, $\tilde{\rho}_{i+1/2} = \frac{\tilde{\rho}_{i+1}+\tilde{\rho}_i}{2}$, and $(\frac{\partial\tilde{\phi}}{\partial\tilde{r}})_{i+1/2} = \frac{\tilde{\phi}_{i+1}-\tilde{\phi}_i}{\Delta\tilde{r}}$.
We note that $\theta = 0$, 0.5, and 1 corresponds to the implicit Euler, Crank-Nicolson, and explicit Euler schemes respectively [6]. We use $\theta = 0.5$ for all of our test calculations so that the entire implicit block is second order in time and space.

The non-linear solver within the implicit block is based on the Jacobian-Free Newton Krylov method [7].

Below, we give a short summary of the Jacobian-Free Newton Krylov method.

The Newton method solves $\mathbf{F}(\mathbf{U}) = 0$ (e.g, assume Eq. (12) is written in this form) iteratively over a sequence of linear system defined by

$$\begin{aligned} \mathbf{J}(\mathbf{U^k})\delta\mathbf{U^k} &= -\mathbf{F}(\mathbf{U^k}), \\ \mathbf{U^{k+1}} &= \mathbf{U^k} + \delta\mathbf{U^k}, \qquad k = 0, 1, \cdots \end{aligned} \tag{14}$$

where $\mathbf{J}(\mathbf{U^k}) = \mathbf{F}'(\mathbf{U^k})$ is the Jacobian matrix and $\delta\mathbf{U^k}$ is the update vector. The Newton iteration is terminated based on a required drop in the norm of the nonlinear residual, i.e,

$$\|\mathbf{F}(\mathbf{U^k})\|_2 < tol_{res}\|\mathbf{F}(\mathbf{U^0})\|_2 \tag{15}$$

where tol_{res} is a given tolerance.

The linear system (14) is solved by the Arnoldi based Generalized Minimal RESidual method (GMRES) which belongs to the general class of the Krylov subspace methods[8]. In GMRES, an initial linear residual, $\mathbf{r}_0$, is defined for a given initial guess $\delta\mathbf{U_0}$,

$$\mathbf{r}_0 = -\mathbf{F}(\mathbf{U}) - \mathbf{J}\delta\mathbf{U_0}. \tag{16}$$

Here we dropped the index k convention since the Krylov (GMRES) iteration is performed at a fixed k. Let j be the Krylov iteration index. The j^{th} Krylov iteration minimizes $\|\mathbf{J}\delta\mathbf{U_j} + \mathbf{F}(\mathbf{U})\|_2$ within a subspace of small dimension, relative to n (the number of unknowns), in a least-squares sense. $\delta\mathbf{U_j}$ is drawn from the subspace spanned by the Krylov vectors, $\{\mathbf{r}_0, \mathbf{J}\mathbf{r}_0, \mathbf{J}^2\mathbf{r}_0, \cdots, \mathbf{J}^{j-1}\mathbf{r}_0\}$, and can be written as

$$\delta\mathbf{U_j} = \delta\mathbf{U_0} + \sum_{i=0}^{j-1}\beta_i(\mathbf{J})^i\mathbf{r}_0, \tag{17}$$

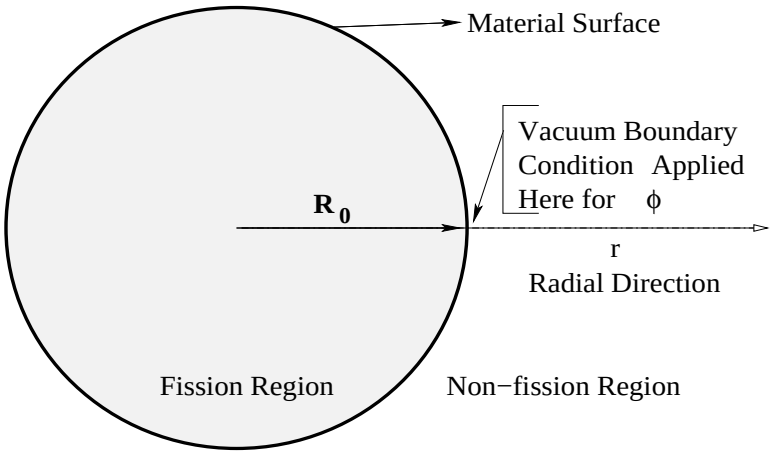

Figure 1. Sketch of a Spherical fission model.

where the scalar β_i minimizes the residual. One particularly attractive features of the GMRES is that it does not require forming the Jacobian matrix. Instead, only matrix-vector multiplications, $\mathbf{J}v$, are needed, where $v \in \{\mathbf{r}_0, \mathbf{J}\mathbf{r}_0, \mathbf{J}^2\mathbf{r}_0, \cdots\}$. This leads to the so-called *Jacobian-Free* implementations in which the action of the Jacobian matrix can be approximated by

$$\mathbf{J}v = \frac{\mathbf{F}(\mathbf{U} + \epsilon v) - \mathbf{F}(\mathbf{U})}{\epsilon}, \tag{18}$$

where $\epsilon = \frac{1}{n\|v\|_2} \sum_{i=1}^{n} b|u_i| + b$, n is the dimension of the linear system and b is a constant whose magnitude is within a few orders of magnitude of the square root of machine roundoff (typically 10^{-6} for 64-bit double precision).

4. RESULTS

In this section, we present our numerical results. The computational example simulates transient behavior of a spherical fast burst reactor. For instance a spherically symmetric fission material is considered (refer to Figure 1).

Given the material, the first step is to evaluate the critical radius. At $t = 0$, we assume constant uniform material density so that we linearize Eq. (7). Then applying the method of separation of variables, we obtain an analytical solution. Considering the first spatial mode of this solution and specified cross sections, we obtain critical radius. For instance, the initial critical material radius, $R_0 = 0.0766m$ for given $\sigma_a = 2.11 \times 10^{-28}m^2, \sigma_f = 1.85 \times 10^{-28}m^2, \sigma_{tr} = 6.80 \times 10^{-28}m^2$, $\nu = 2.98$, and $v = 10^5 m/sec$ (these cross sections belong to ^{239}Pu [9]). We note that slightly changing parameters (e.g, increasing the initial radius or increasing ν) is equivalent to inserting reactivity and results supercritical reactor state.

Initially, the reactor is set to a supercritical state. This leads to power rise consequently temperature rise. Then the rising temperature causes the material to expand leading to a density drop. Decreasing density results in an increase in neutron leakage therefore turning the reactor into subcritical state. Further in time, reactor shuts itself down because the material stays in expanded state due to lack of heat extraction mechanism in our model.

The initial and boundary conditions for the field variables are set as follows; The initial neutron flux is set to, $\tilde{\phi}(\tilde{r}, 0) = C_\phi \frac{\sin \pi \tilde{r}}{\tilde{r}}$ where C_ϕ is determined by the power formula, i.e,

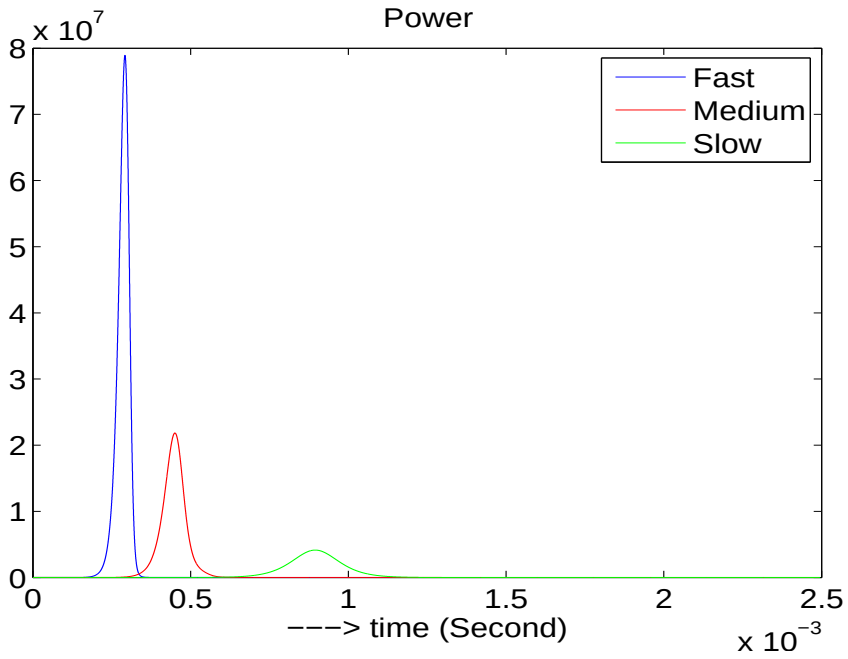

Figure 2. Power pulses (Watt) from the coupled model.

$P = E_R \Sigma_f \int \tilde{\phi}(\tilde{r}, 0) dV$ with E_R being the recoverable energy per fission (typically, $E_R = 3.2 \times 10^{-11} J$). The boundary conditions for ϕ are the symmetry condition at $\tilde{r} = 0$, i.e, $\nabla \tilde{\phi} = 0$ and the vacuum boundary condition near $\tilde{r} = 1$, i.e, $\tilde{\phi} = 0$ at some small distance near the material surface (in many practical applications this distance is negligibly small). The non-dimensional initial temperature is 1. For the temperature, we apply symmetry boundary condition at the center, and a second order extrapolation boundary condition at the material surface. The initial displacement is set to *zero*. At the center of the sphere, we set symmetric displacement , and at the material surface we use Eq. (10). The initial density is set as $\rho_0 = 19.7 \times 10^3 kg/m^3$. The boundary conditions for the density is set via Eq. (4). The other material parameters are set as $\epsilon = 1.0 \times 10^{11} Pa$, $\upsilon = 0.15$, $\beta = 53 \times 10^{-6} K^{-1}$, and $c_p = 13 J/kgK$.

In this paper, we tested three different reactivities/power pulses and observed the material responses accordingly. In all three cases, $R_0 = 0.078m$ so that we have supercritical reactor state. To achieve different levels of reactivity, we adjusted neutron production term (i.e, $\nu = 2.98, 2.95,$ and 2.93 for a fast, medium, and slow pulse). The initial power is set to *one*.

We note that the time scales for neutronics and the elastic wave are $\tau^{neutron} = \frac{l}{k-1}$ and $\tau^{elastic} = \frac{R}{c}$ so that $\frac{1}{\tilde{c}} = \frac{\tau^{elastic}}{\tau^{neutron}}$ in Eq. (9).

Figure 2 shows a fast, medium, and slow power pulse (we used $M = 50$ mesh points for these computations). The corresponding material responses are shown in Figure 3. The time scales behave as $\tau^{neutron} < \tau^{elastic}$ for the fast pulse and $\tau^{elastic} < \tau^{neutron}$ for the slow pulse (refer to Figure 4). We see significant material vibrations for the fast pulse, this is because the material doesn't have enough time to respond to the fast power rise. On the other hand, we don't see any vibration for the slow power test since the material can respond to the slow power rise with a non-vibrating expansion.

These behaviors can be derived from the mathematical equations. Indeed, if we rewrite Eq. (9) in terms of the two time scales, we have

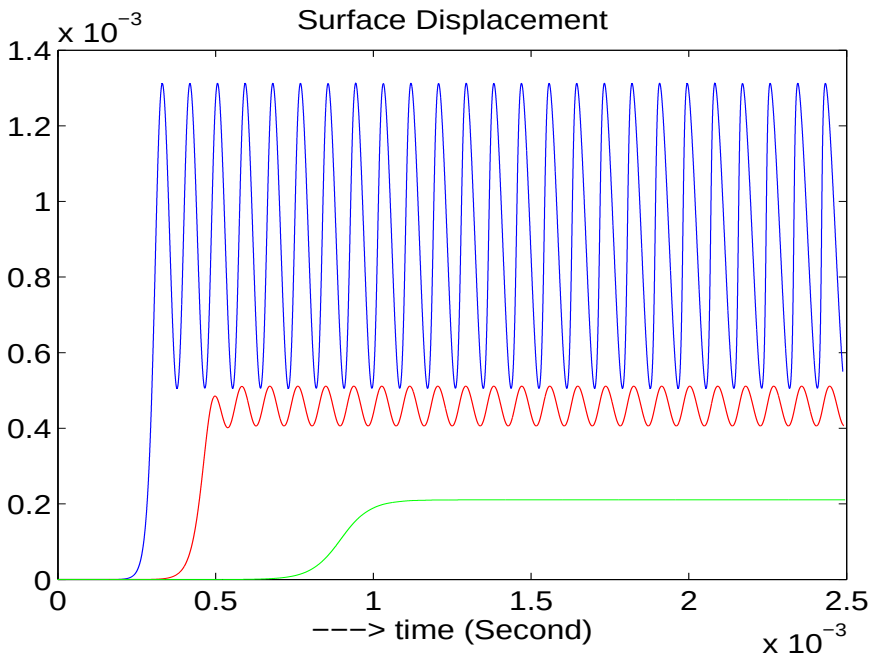

Figure 3. Surface displacements (Meter) corresponding to the power pulses in Figure 2.

$$(\frac{\tau^{elastic}}{\tau^{neutron}})^2\frac{\partial^2\tilde{u}}{\partial^2\tilde{t}} - [\frac{\partial^2\tilde{u}}{\partial^2\tilde{r}} + \frac{2}{\tilde{r}}\frac{\partial\tilde{u}}{\partial\tilde{r}} - \frac{2}{\tilde{r}^2}\tilde{u}] + \frac{1+\upsilon}{1-\upsilon}\beta T_0\frac{\partial\tilde{T}}{\partial\tilde{r}} = 0. \tag{19}$$

For the fast pulse, $1 << (\frac{\tau^{elastic}}{\tau^{neutron}})^2$ meaning Eq. (19) supports a wave structure. On the other hand, $(\frac{\tau^{elastic}}{\tau^{neutron}})^2 << 1$ for the slow pulse in which case the time term in Eq. (19) is insignificant.

At this point Eq. (19) doesn't support a wave structure anymore leading to a flat displacement profile. Thus, by non-dimensional analysis of the coupled system we can observe the limits and shed light on conditions required to observe vibration. The medium strength power pulse results in moderate material vibrations.

The core of this study was our non-dimensional mathematical analysis to explain certain material behaviors which are experimentally observed. However, our solutions are obtained from a numerical model, therefore it requires some verifications, especially, concerning the time discretization.

To verify the time accuracy of our numerical procedure, we carried out a numerical convergence analysis. To measure the time convergence, we run the code with a fine mesh (e.g, $M = 400$ points) and different time step refinements to a final time (e.g, $t_{final} = 1.5 \times 10^{-4}$). Then we measure the L_2 norm of errors between *two* consecutive time step runs and observe the rate of decrease in these errors. For instance, Figure 5 shows the second order time convergence of the scheme for Neutron flux and displacement. We have provided further numerical convergence analysis (e.g, regarding the spatial accuracy) and a partial analytical verification in [4].

We would like to make some remarks about the solver performance. The implicit solver converges to a given tolerance with on average *three* Krylov iterations and *one* Newton step in smooth regions. On the other hand, in high gradient regions (e.g, where there is a steep power rise), the convergence takes on average 35 Krylov iterations and *two* Newton steps. We note that the code performance can be improved by preconditioning the Krylov block.

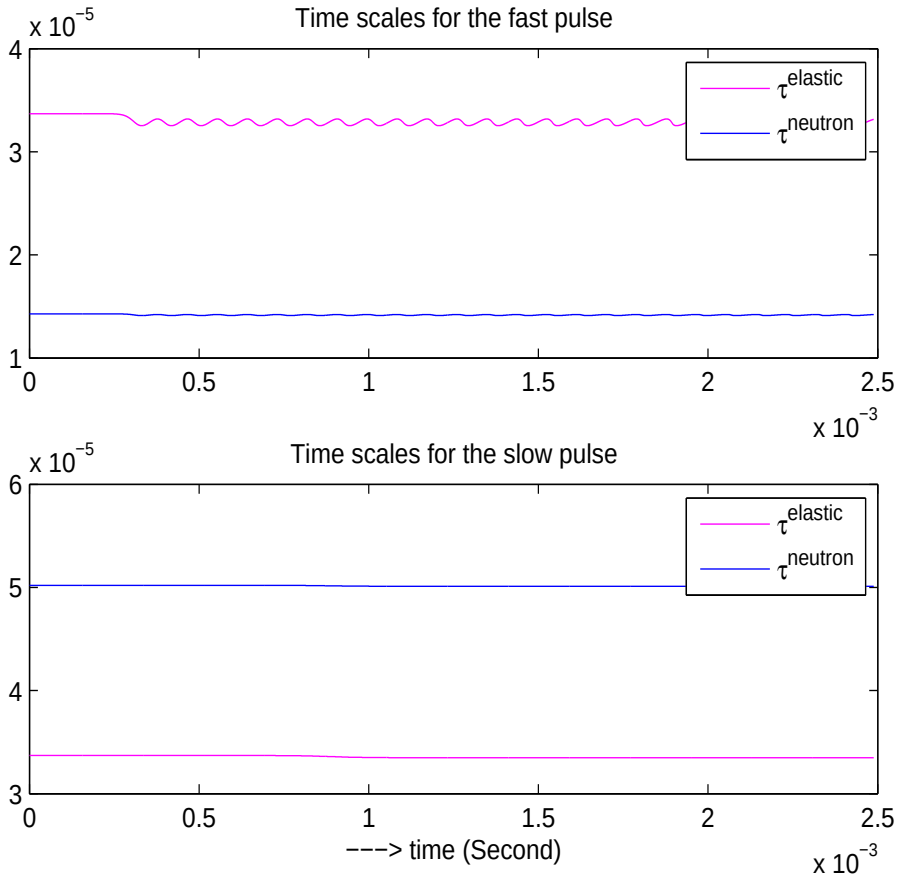

Figure 4. Elastic and neutron time scales for the fast and slow power pulses (e.g, refer to Figure 2).

5. CONCLUSIONS

We have presented a preliminary study for the coupling of neutron diffusion and thermomechanics of fast burst reactors. We illustrated the mechanical response of the material to different power (reactivity) settings. We showed that if there is a fast power rise in the system, then the material expands to a certain level and starts vibrating. On the other hand, if the power slowly increases, then the material expands with significantly less or non-vibrating fashion. Analysis of the non-dimensional system illuminates the distinct physical regimes which are observed.

Our future work involves making use of the transport theory for solving neutronics and coupling it with an hydrodynamics model to solve the material properties.

ACKNOWLEDGEMENTS

The submitted manuscript has been authored by a contractor of the U.S. Government under Contract No. DEAC07-05ID14517 (INL/CON-08-15004). Accordingly, the U.S. Government retains a non-exclusive, royalty-free license to publish or reproduce the published form of this contribution, or allow others to do so, for U.S. Government purposes.

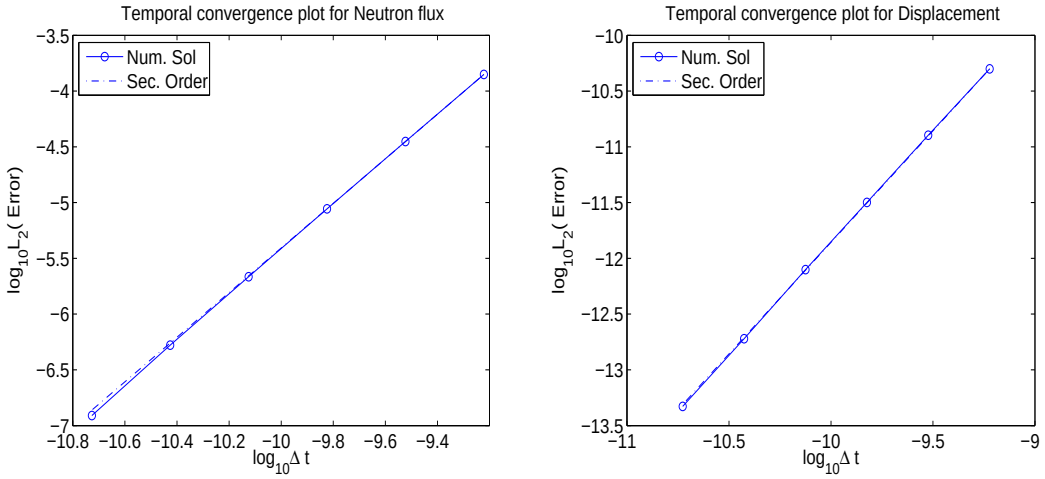

Figure 5. Temporal convergence analysis for neutron flux and displacement.

REFERENCES

[1] D. Burgreen, “Thermoelastic Dynamics of Rods, Thin Shells, and Solid Spheres”, *Nuclear Science and Engineering*, **12**, pp. 203-217 (1962).

[2] S. C. Wilson and S. R. Biegalski, “Computational Modeling of Coupled Thermomechanical and Neutron Transport Behavior in a Godiva-Like Nuclear Assembly”, *Nuclear Science and Engineering*, **157**, pp. 344-353 (2007).

[3] J. J. Duderstadt and L. J. Hamilton, *Nuclear Reactor Analysis*, John Wiley & Sons, Inc, (1976).

[4] S. Y. Kadioglu, D. A. Knoll and C. Oliveria, ”Multi-physics Analysis of Spherical Fast Burst Reactors”, *Nuclear Science and Engineering*, under review, (submitted in December 2008).

[5] R. J. Leveque, *Finite Volume Methods for Hyperbolic Problems*, Cambridge University Press, Texts in Applied Mathematics, (1998).

[6] J. W. Thomas, *Numerical Partial Differential Equations I (Finite Difference Methods)*, Springer-Verlag New York, Texts in Applied Mathematics, (1998).

[7] D. A. Knoll and D. E. Keyes, ”Jacobian-Free Newton Krylov Methods: a survey of approaches and applications”, *J. Comput. Phys.*, **193**, pp. 357-397 (2004).

[8] Y. Saad, *Iterative Methods for Sparse Linear Systems*, Siam, (2003).

[9] J. R. Lamarsh and A. J. Baratta, *Introduction to Nuclear Engineering*, Prentice Hall (2001).